Applied Catalysis B: Environmental 134–135 (2013) 145–152

Contents lists available at SciVerse ScienceDirect

Applied Catalysis B: Environmental

journal homepage: www.elsevier.com/locate/apcatb

Au/carbon as Fenton-like catalysts for the oxidative degradation of bisphenol A

Xuejing Yang[a], Peng-Fei Tian[a], Chengxi Zhang[b], Ya-qing Deng[a], Jing Xu[a], Jinglong Gong[b], Yi-Fan Han[a,*]

[a] State Key Laboratory of Chemical Engineering, East China University of Science and Technology, Shanghai 200237, People's Republic of China
[b] Key Laboratory for Green Chemical Technology of Ministry of Education, School of Chemical Engineering and Technology, Tianjin University, Tianjin 300072, People's Republic of China

ARTICLE INFO

Article history:
Received 14 September 2012
Received in revised form 2 January 2013
Accepted 4 January 2013
Available online 16 January 2013

Keywords:
Heterogeneous Fenton catalyst
Au catalysts
Active carbon
Degradation of bisphenol A

ABSTRACT

The development of a new method for the degradation of bisphenol A (BPA) in aqueous solution is highly desired. Oxidative degradation using hydroxyl radicals (OH•) is an efficient approach for the remedy of toxic organic compounds. This paper describes the design and utilization of a new Fenton system consisting of the Au/styrene based activated carbon catalyst and hydrogen peroxide (H_2O_2) for the degradation of BPA under non-photo-induced conditions. Transmission electron microscopy (TEM), X-ray diffraction (XRD) and X-ray photoelectron spectroscopy (XPS) results showed that the negatively charged Au nanoparticles were evenly distributed in a range 3.9–6.4 nm dominated with (1 1 0) facet. The generation of OH• over Au catalysts through the decomposition of H_2O_2 was evidenced using 5,5-dimethyl-1-pyrroline-N-oxide (DMPO) trapped electron paramagnetic resonance (EPR). The experimental results suggested that the conversion of BPA was affected by several factors such as the loading amount of Au, pH value, reaction temperature and the initial concentration of H_2O_2. In an optimum experiment, BPA could be degraded from 110 to 10 ppm within 12 h. The active sites was envisaged to be negatively charged Au atoms at the interface between Au particles and carbon support, the carbon surface is enriched with dangling carbon atoms as evidenced by the O_2-temperature programmed desorption (TPD) technique. A mechanism including the redox between $Au^{\delta-} \leftrightarrow Au^{\circ}$ during the decomposition of H_2O_2 has been proposed.

1. Introduction

Bisphenol A (BPA; 2,2-bis-(4-hydroxy phenyl)-propane) is regarded as a potential "endo-crinedisruptor" by the US Environmental Protection Agency (EPA) [1]. Up to date, most of studies on the environmental issues caused by BPA have been contributed to the occurrence, ecological risk, estrogenic activity and the effects on the health of human and animals. As an additive or contaminate, BPA can be detected in food [2], water [3], paper (including paper products, currencies, etc.) [4] and plastic products [5]. It has shown the effects of estrogen-like on gene imprinting and sexual differentiation when accumulating in human body [6]. The degradation of BPA naturally needs more than 90 years [7]. That means the pollution resulted from BPA or other chemicals with similar structure can last for several decades once it is released into water or soil [6]. Presently, several methods have been developed for the removal of BPA from aqueous solution, for instance, biochemical oxidation, absorption, electrochemical oxidation, wet chemical oxidation, ozonation, sonochemical oxidation and so forth [8–16]. The biodegradation approach, as a process widely used in industrial scale, needs several weeks or longer [12]. Therefore the development of a fast and simple method for the degradation of persistent organic compounds, especially for BPA, is still a tremendous challenge. Among all these methods, Fenton system shows the highest efficiency in the oxidation of organic compounds. In addition, as a model organic contaminate, BPA can be a category of organic compounds with benzyl rings, which is still difficult to be removed by the conventional methods.

The Fenton process as an advanced oxidation process (AOP) has long been used for the remedy of waste water and contaminated soil [17]. According to the radical (Weiss–Harber) mechanism, hydrogen peroxide (H_2O_2) can be decomposed into hydroxyl radical (•OH) by ferrous ions catalyst. •OH has the second highest oxidant potential (2.7 eV in an acidic solution) in nature and can oxidize organic compounds in aqueous rapidly [18–20]. However, the cost for this process could be too high in practical application because of the production of undisposable sludge, the continuous lost of the chemicals (mainly iron salt) and the narrow range of operation pH value (2.5–3.5) [21]. Nowadays, the heterogeneous Fenton agent was indicated as an ideal solution to these problems

* Corresponding author. Tel.: +86 21 64251928; fax: +86 21 6425192.
E-mail address: yifanhan@ecust.edu.cn (Y.-F. Han).

0926-3373/$ – see front matter © 2013 Elsevier B.V. All rights reserved.
http://dx.doi.org/10.1016/j.apcatb.2013.01.008

[22,23]. Solid iron-based catalysts [24] have showed comparable catalytic performance to the conventional Fenton catalyst (Fe^{2+}); however, the leaching of iron generally leads to a significant deactivation. Therefore, the development of novel heterogeneous Fenton system with enhanced stability is strongly desired, it would be of great importance for both environmental protection and chemical synthesis.

Au catalysis attracts tremendous attention since the seminal discovery on the superior performance of Au nanoparticles in 1980s [25,26]. Au-based catalysts have proven active for low-temperature oxidation, hydrogenation, water–gas shift, electrochemical reaction and so forth [27–34]. We have reported that Au/hydroxyapatite could be an alternative Fenton-like catalyst, which degrades H_2O_2 to •OH [35]. More recently, Garcia's group [36–39] has reported that a nanodiamond supporting Au (Au/OH-npD diamond) could be a Fenton catalyst for the metabolism of organic compounds under light irradiation [36]. The reaction was assumed to proceed through a photochemical process including a photo-induced electron ejection on the catalyst surface and the electron-transfer from Au to H_2O_2 [37]. Indeed, Au atoms can be excellent electron-donor or -acceptor under certain circumstances; in particular, this property can be used for the production of •OH by H_2O_2 decomposition. Au-Fenton catalysts have a great advantage compared to solid Fe-Fenton catalysts because Au is "inert" in nature and unlikely leaching under various reaction conditions.

In this study, Au nanoparticles dispersed on various carbon supports were prepared, characterized and used as solid Fenton catalysts for the degradation of BPA under mild conditions. In particular, the origin of active sites over Au/C catalyst was explored using multi techniques.

2. Experimental

2.1. Synthesis of the carbon material

2.1.1. Styrene-based activated carbon (SRAC)

A commercial polystyrene-based ion-exchange resin sphere (Rohm & Haas, USA) was used for the preparation of SRAC. Generally, it was carbonizated at 1073 K for 2 h in gaseous N_2, followed with an activating process at 1073 K for 60 min in water stream.

2.1.2. Pitch-based spherical activated carbon (PSAC)

The preparation of PSAC was followed the method introduced by Liu et al. [40]. Coal tar pitch was purified by HCl, and stabilized with 30 wt% naphthalene.

The obtained spheres were then carbonized at 1173 K for 0.5 h with a ramping rate of 10 K/min in a flow of N_2. The carbonized materials were activated at 1173 K for 2 h in a steam of 30 mL/min.

2.1.3. Carbon nanofiber (CNF)

A chemical vapor deposited (CVD) method was used for the preparation of CNF. A Ni/Al_2O_3 catalyst was selected for this system, and CO/H_2 (80/20) mixed gas flow was the carbon source. After 16 h for the nanofiber growth, the purification of the obtained materials was carried out with the concentrated NaOH.

2.1.4. Ordered mesoporous carbon (FDU-15)

The route for the synthesis of FDU-15 was followed the method proposed by Meng et al. [41]. Hexadecane and decane (a mole ratio of 1.55) was used as the source of carbon. After blending for 24 h at 338 K, the slurry precursor was obtained. Then, it was vacuum dried. With the ramping rate of 1 K/min to 623 K, the sample was calcined in N_2. Finally, the carbonized was carried out at 1073 K in a N_2 flow of 30 mL/L for 3 h.

2.2. Preparation of the catalyst

The introduction of Au nanoparticles followed the same procedure [42]. $Au(en)_2Cl_3$(en: 1,2-ethanediamine) was employed as the precursor, which could be adsorbed to SRAC at room temperature with pH 3.0. The obtained samples were washed with MilliQ (18.25 MΩ) water and then dried at 313 K overnight. The heat treatment was proceeded subsequently at 573 K in a H_2 flow of 30 mL/min for 30 min. The obtained catalyst was sealed in a dark vessel.

2.3. Catalytic test

The aqueous solution of BPA (~100 ppm) was prepared with MilliQ water (18.25 MΩ). The pH value was adjusted using 0.01 M HCl. The catalyst was added into the solution after forming a mixture of BPA, H_2O_2 and HCl in a thermostatic batch reactor. The reactor was tightly covered by aluminum foil for the evaluation of the influence of solar-light. In all the cases, aliquots of 2 mL were taken at interval of 1 h, and filtered by a 0.22 μm nylon membrane before analysis. The concentration of BPA was measured by a HPLC (Perkin Elmer Flexar) that was equipped with a Spheri-5 C18 column and UV detector with the wavelength 275 nm [10]. The variation of H_2O_2 concentration during reaction was analyzed colorimetrically using a UV–vis spectrophotometer after complexation with a $TiOSO_4/H_2SO_4$ reagent [43].

2.4. Characterization

2.4.1. Scanning electron microscopy (SEM)

The measurements were carried out at a FEI NOVA NanoSEM 450 scanning electron microscopy, which was operated at the accelerating voltage of 15 kV and the detector current of 10 mA. The collection was taken at a high vacuum mode (1×10^{-3} mbar). The size of the beam spot was 3 μm.

2.4.2. N_2 adsorption–desorption

N_2 adsorption and desorption isotherms were collected on a ASAP 2010 (Micromeritics, USA) at 77 K. Prior to the measurement, all samples were degassed at 573 K until a stable vacuum of ca. 5 m Torr was reached. The pore width distribution curves were calculated from the adsorption branch using a DFT method. The specific surface area was assessed using the BET method from adsorption data in a relative pressure range from 0.06 to 0.35. The conversion factor between the volume of gas and liquid adsorbate is 0.0015468 for N_2 at 77 K, when they are expressed in cm^3/g and cm^3 STP/g, respectively.

2.4.3. X-ray diffraction (XRD)

XRD was performed using Riguku D/max 2550 diffractometer, with accelerated voltage 40 kV and detector current 100 mA. Cu-K_α radiation was used for a continuous scanning with the step-size of 0.02° over a 2θ range 10–80°. The scan speed was 4°/min.

2.4.4. Transmission electron microscopy (TEM)

The measurements were performed on a JEOL-2000, which was operated at 200 kV accelerating voltage. The catalyst was first carefully grounded at an agate mortar to 30 μm. Then the fine sample was ultrasonically suspended in ethanol. One drop of this slurry was deposited on a copper microgrid without carbon coating. The liquid phase was evaporated before the grid was loaded into the microscope. The Au particle size was estimated on the basis of 300 particles.

2.4.5. X-ray photoelectron spectroscopy (XPS)

The analysis was performed on a PHI 1600 spectrometer, using Mg-K_α radiation (1253.6 eV, passing energy 29.3 eV). The base pressure of the instrument is about 1×10^{-9} Torr. The background contribution B (E) (obtained by the Shirley method) caused by inelastic process was subtracted, while the curve-fitting was performed with a Gaussian–Lorentzian profile by a standard software. The binding energies (BEs) were calibrated by using C_{1s} peak at 284.6 eV as references. The instrument was also calibrated by using Au foil (Au $4f_{7/2}$ at 84.0 eV).

2.4.6. 5,5-Dimethyl-1-pyrroline-N-oxide (DMPO) trapped electron paramagnetic resonance (EPR)

The DMPO trapped EPR spectrums of Au/SRAC and SRAC were carried out at a Bruke EMX-8/2.7 C electron paramagnetic resonance spectroscopy, which was operated at X-field with a center field at 3511.520 G. And the sweep width was 200 G. The microwave frequency was 9.873 GHz, and power was 2.015 mW. Sweep time of the signal channel was 41.9 s, with a 3.56×10^4 gain at the receiver. Before the test, 50 mg of SRAC, Au(1.5 wt%)/SRAC, Au(3.0 wt%)/SRAC were added into 200 mL solution containing 500 ppm H_2O_2 with a pH of 3.0, respectively. After stirring for 2 min and subsiding for 1 min, 1 mL aliquots was taken and ejected to 1 mL DMPO (Sigma–Aldrich, 100 ppm diluted by MilliQ water) immediately. The obtained solution was transferred to a 100 μL capillary tube, which was then fixed in the resonant cavity of the spectrometer.

2.4.7. O_2-temperature programmed desorption (TPD)

Before adsorption to saturation by oxygen pulse, the sample (0.01 g) was degassed at 573 K in Ar flow for 30 min and then cooled down to 213 K in He. It was then purged by N_2 for 30 min, the desorption of oxygen was monitored by a Micromeritics AUTOCHEM II 2920 system, the intensity of $m/z = 32$ was recorded with a ramping rate of 10 K/min to 873 K in a He flow of 20 mL/min.

2.4.8. Inductively coupled plasma mass spectrometry (ICP-MS)

The sample was added to 10 mL mixture of H_2SO_4 (37.5%) and HCl, following with microwave digestion. The solution was then diluted with MilliQ water, Au was measured using a Perkin Elmer NexION 300 ICP-MS.

3. Results and discussion

3.1. Activities of BPA degradation over supported gold catalysts

The activities of the carbon-supported catalysts for BPA degradation were obtained in an acidic solution (pH 3.0). Moreover, commercial gold catalysts (provided by the world gold council) were evaluated under the same experimental conditions as well. As summarized in Table 1, about 89% of BPA can be degraded at 313 K over Au(3.0%)/SRAC, which exhibited the best performance among all the catalysts. The performance of Au/SRAC is comparable with that of Au/OH-npD diamond reported by Martín et al. without the assistant of photo [38], because the reaction rate constants of •OH toward phenol ($\sim 1.0 \times 10^{10}$ min^{-1}) and BPA (0.9×10^{10} min^{-1}) in the homogeneous system were very closed [44]. According to the results shown in Fig. 1, the effect of solar-light can be negligible. The uniform of the particle size may be the key factor in comparison to other Au/C catalysts. Previous studies have revealed [21–30] that the size of Au nanoparticles is of great importance to the catalytic activity. Additionally, for the heterogeneous Fenton reaction, the produced radicals can be scavenged rapidly by H_2O_2, intermediates and support materials. The unique properties of SRAC may be responsible for the superior performance of the obtained catalyst.

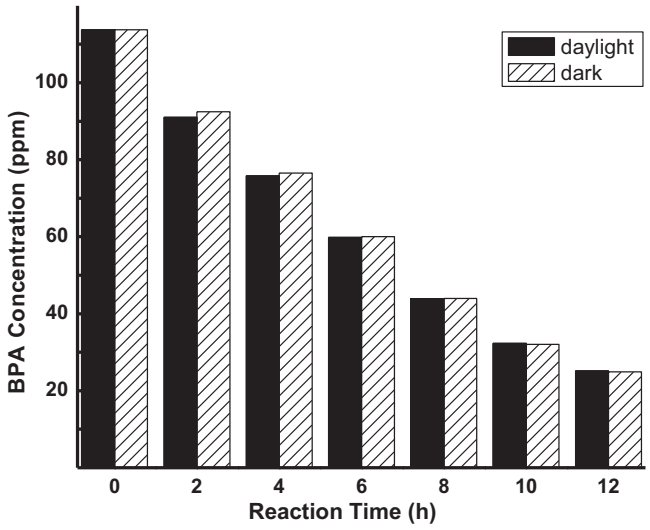

Fig. 1. Comparison of catalytic activity in daylight (full filled) and dark (with slash). Reaction condition: 313 K, pH 3.0, initial [BPA] = 113 ppm, [H_2O_2] = 530 ppm, Au(1.5 wt%)/SRAC 125 mg/L and 12 h.

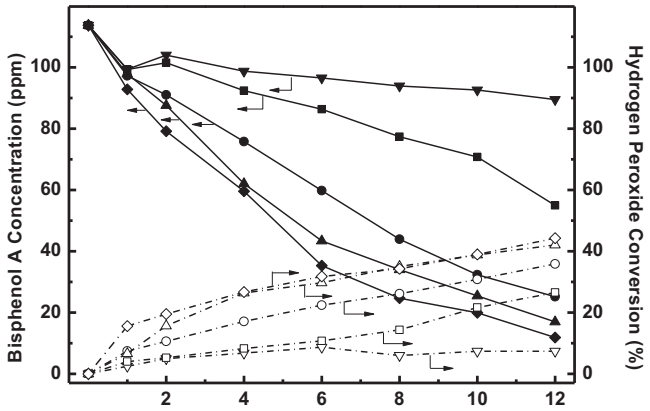

Fig. 2. Degradation of BPA (solid line) and the decomposition of H_2O_2 (dotted line) over SRAC supported gold catalysts with different loading amount: 0.0% (▼, ▽); 1.0% (■, □); 1.5% (●, ○); 2.0% (▲, △); 3.0%(♦, ◊). Reaction condition: Au/SRAC 125 mg/L, 313 K, $[BPA]_{initial}$ = 89 ppm, $[H_2O_2]_{initial}$ = 530 ppm, pH 3.0.

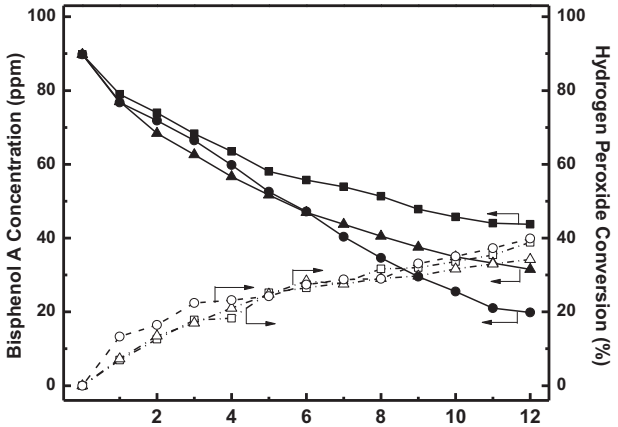

Fig. 3. Influence of pH value on the degradation of BPA (solid line) and the decomposition of H_2O_2 (dotted line): pH 7.0 (■, □); pH 5.0 (▲, △); pH 3.0 (●, ○). Reaction condition: Au(1.5 wt%)/SRAC 125 mg/L, 313 K, $[BPA]_{initial}$ = 89 ppm, $[H_2O_2]_{initial}$ = 530 ppm.

Table 1
Activities of support Au catalysts for the degradation of BPA. Reaction Conditions: initial [BPA] = 114 ppm, [H_2O_2] 530 ppm, 313 K, pH 3.0, catalyst 125 mg/L, and reaction time 12 h.

Entry	Catalysts	Size (nm)	BPA Conv. (%)	H_2O_2 Conv.(%)
1	Au/SRAC (3.0 wt%)	4.4[b]	89.0	44.1
2	Au/PSAC (3.0 wt%)	15.1[b]	23.8	8.3
3	Au/CNF (3.0 wt%)	16.8[c]	20.4	14.5
4	Au/FDU-15 (3.0 wt%)	11.3[c]	32.4	22.8
5	Au/X40s[a] (10.0 wt%)	10.5	14.5	10.7
6	Au/Fe_2O_3[a] (5.0 wt%)	4.0	10.1	7.6
7	Au/TiO_2[a] (1.5 wt%)	3.5	5.3	10.8
8	Au-Fe_2O_3/Al_2O_3[a] (0.5 wt%)	2.8	6.6	15.3

[a] Gold reference catalysts from world gold council.
[b] Average particle size from TEM images.
[c] Particle size calculated from XRD peaks broadening of Au(1 1 1) by the Sherr equation.

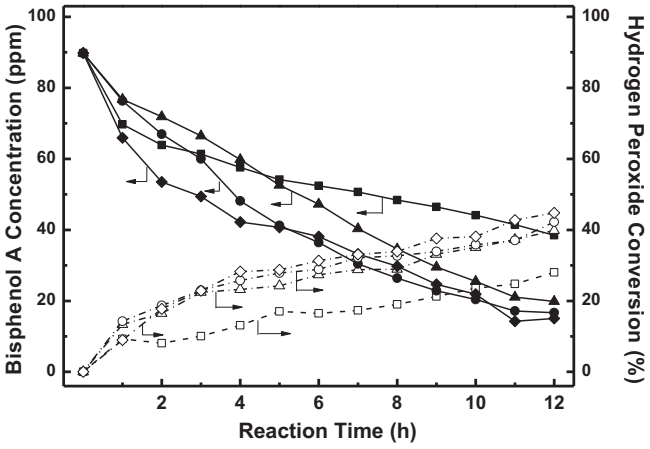

Fig. 4. Influence of temperature on the degradation of BPA and the decomposition of H_2O_2: 303 K (■, □); 313 K (▲, △); 323 K (●, ○); 333 K (♦, ◊) Reaction condition: Au(1.5 wt%)/SRAC 125 mg/L, pH 3, $[BPA]_{initial}$ = 89 ppm, $[H_2O_2]_{initial}$ = 530 ppm.

3.2. Au loading amount

In the following section, the activity of Au/SRAC catalyst was tested under different conditions. The influence of Au loading amount, temperature, pH value and the addition of H_2O_2 was evaluated. As shown in Fig. 2, the BPA conversion and the decomposition

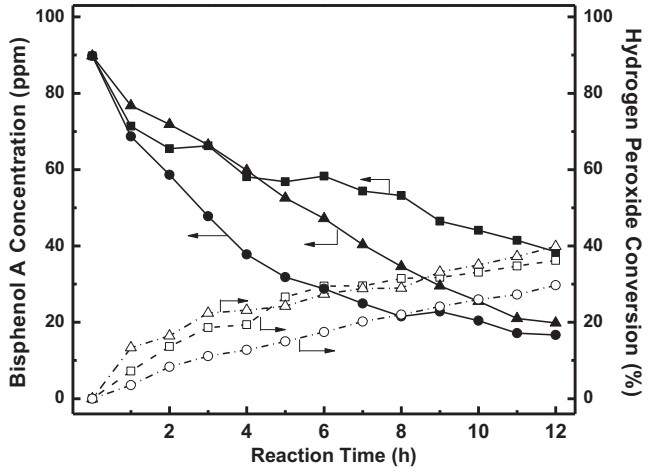

Fig. 5. Influence of H_2O_2 concentration on the degradation of BPA (solid line) and the decomposition of H_2O_2 (dotted line): 275 ppm (■, □); 530 ppm (▲, △); 835 ppm (●, ○). Reaction condition: Au(1.5 wt%)/SRAC 125 mg/L,313 K, pH 3, $[BPA]_{initial}$ = 89 ppm.

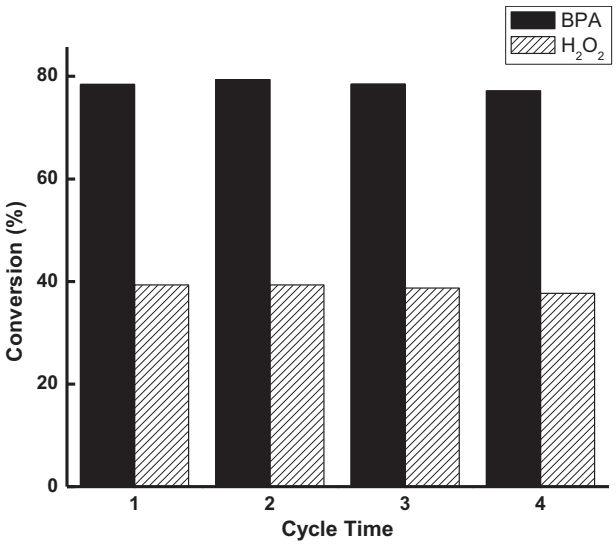

Fig. 6. Degradation of BPA (full filled) and H_2O_2 (with slash) after several cycles on the Au(1.5 wt%)/SRAC catalyst.

of H_2O_2 were increased with the rise of Au content simultaneously. The bare carbon exhibited almost no activity toward the degradation while a small amount of BPA (less than 10%) could be adsorbed initially. The BPA concentration was decreased from initial 114 to 12.5 ppm after 12 h over a Au(3.0 wt%)/SRAC catalyst at pH 3 and 313 K.

3.3. pH value

In the subsequent study, the Au(1.5 wt%)/SRAC catalyst was used if without emphasis. This reaction is favored under strong acidic conditions (pH 3) and a moderate activity was observed even in a neutral solution (Fig. 3). The conversions of H_2O_2 at different pH values are approximately identical. This probably indicates that the productivity of •OH is more favorable in acidic solutions.

3.4. Temperature

The conversion could be slightly low at 303 K but increased rapidly with increasing the temperature from 313 to 333 K (Fig. 4).

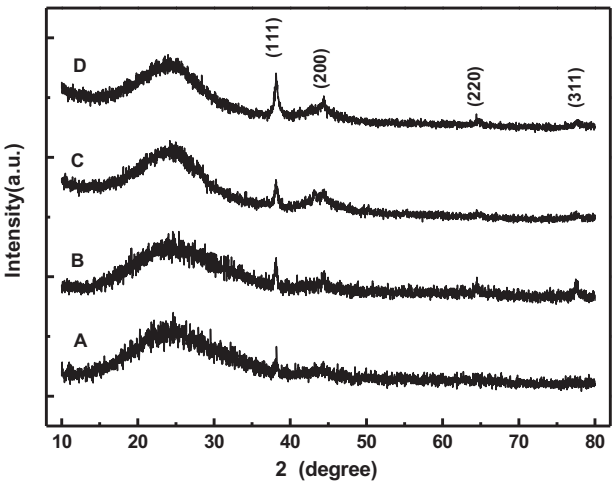

Fig. 7. XRD patterns of Au/SRAC catalysts. (A) Au(1.0 wt%)/SRAC, (B) Au(1.5 wt%)/SRAC, (C) Au(2.0 wt%)/SRAC, (D) Au(3.0 wt%)/SRAC.

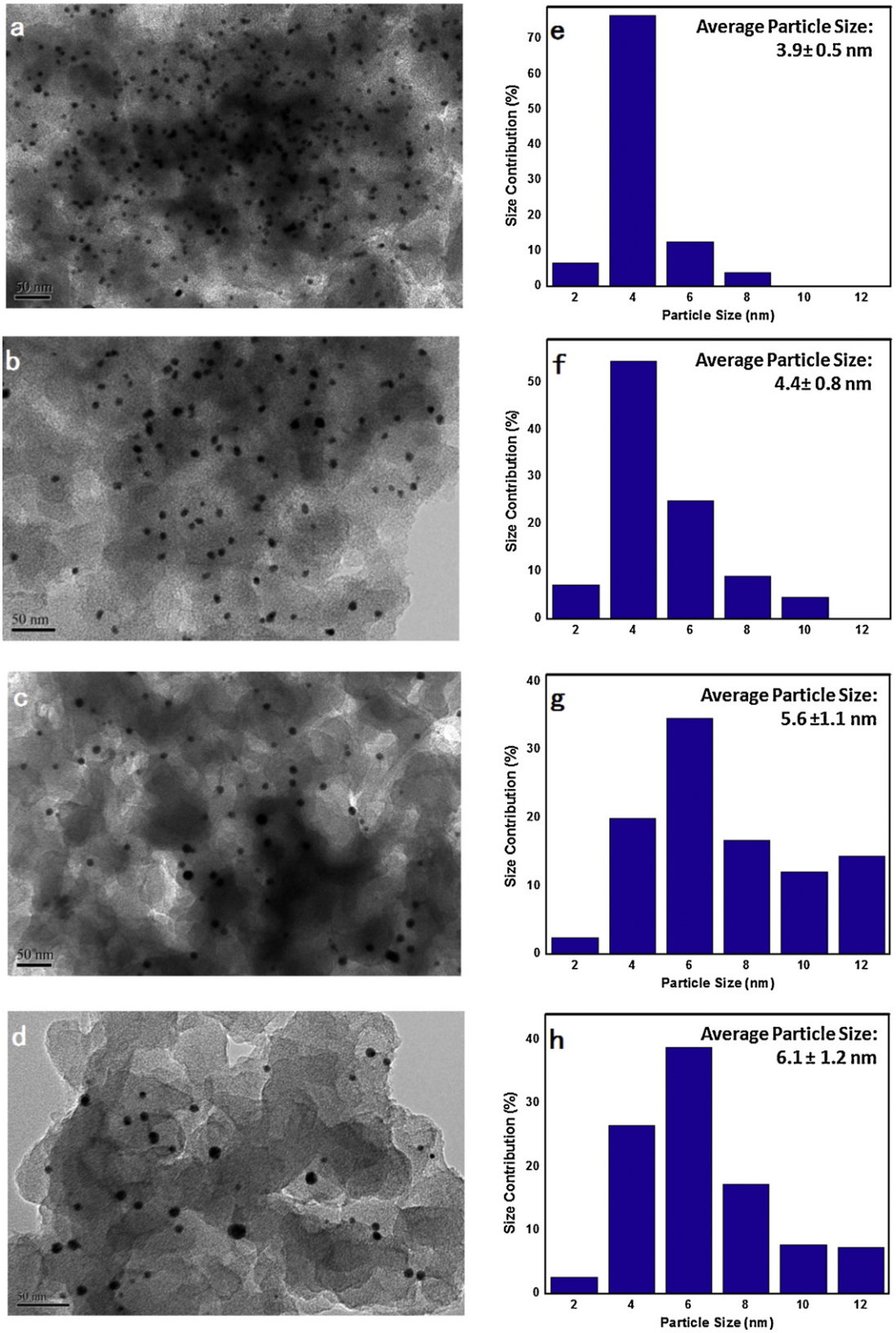

Fig. 8. TEM images and size distributions of Au/SRAC catalyst with different loading amount. (a, e) Au(1.0 wt%)/SRAC, (b, f) Au(1.5 wt%)/SRAC, (c, g) Au(2.0 wt%)/SRAC, (d, h) Au(3.0 wt%)/SRAC.

After running 12 h, the conversion of BPA increased from 20% to 38% with varying the temperature from 303 to 313 K. The degradation of BPA could not be accelerated with further increasing the temperature.

3.5. H_2O_2 initial concentration

The degradation reaction could also be enhanced with an increase in the initial H_2O_2 concentration (Fig. 5). The

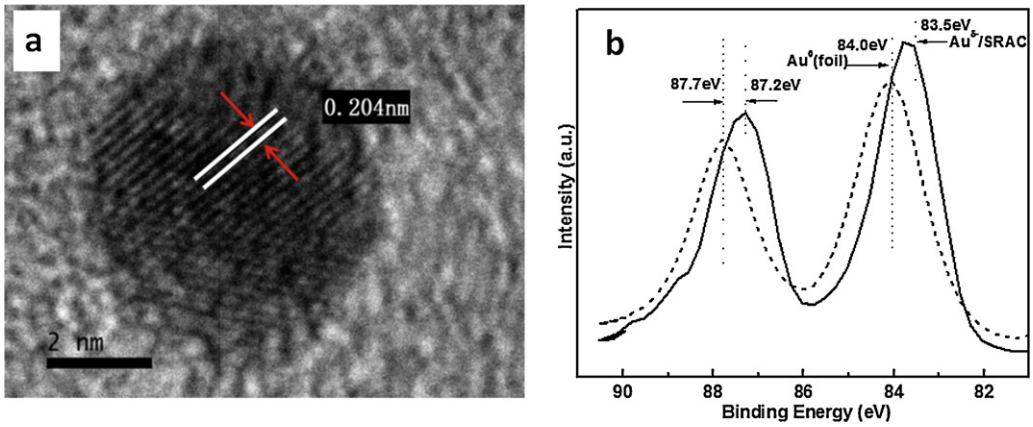

Fig. 9. (a) HRTEM of a single particle from Au(1.5 wt%)/SRAC, (b) XPS Au_{4f} spectra of Au(1.5 wt%)/SRAC (solid line) and Au foil (dotted line).

decomposition of H_2O_2 decreased from 40% to less than 35% when the concentration of H_2O_2 increased from 530 to 835 ppm. Meanwhile, the conversion of BPA was also increased about 4%. The addition of oxidant was no doubt caused the feasibility between active center and reactant. However, the existence of H_2O_2 also served as a medium scavenger (2×10^7 min^{-1}) with large population. Further raising the H_2O_2 concentration moderately increased the conversion of BPA.

3.6. The stability of the catalyst

It is noted that the catalyst can be recycled for several times without deactivation in a strong acidic solution (pH 3.0, Fig. 6). The loss of activity is probably due to the deterioration of reactive sites, which is caused by the complexing or adsorption of byproducts and the configuration evolution of the active species during reaction. In the case of this study, the relative inertia of nano Au led to the superior stability of the catalyst. A great potential of Au Fenton catalyst was exhibited even though the cost of Au Fenton is higher than that for the traditional Fenton agent.

3.7. Structure of Au/SRAC catalysts

XRD patterns (Fig. 7) and TEM images (Fig. 8) showed Au nanoparticles were evenly dispersed on the surface of SRAC. The diffraction peaks of the facet of Au [1 1 1], [2 0 0], [2 2 0] and [3 1 1] can be observed in a broad diffraction peak related to the graphite structure of activated carbon. The average particle size increases from 3.9 ± 0.5 nm to 6.4 ± 1.2 nm with rising the Au content from 1.0 wt% to 3.0 wt%. In the case of Au(1.5 wt%)/SRAC, the average size of Au particles was estimated to be 4.4 ± 0.8 nm with irregular shape (Fig. 8a), while the HRTEM image (Fig. 9a) demonstrated that Au(1 0 0) was a predominant facet in Au crystalline. XPS spectra (Fig. 9b) indicated that Au nanoparticles were negatively charged or partial polarized because the binding energy (BE) of Au 4f shifted down by ca. 0.3 eV.

3.8. DMPO trapped EPR and O_2-TPD

To explore the origin of active sites in Au/SRAC, spin trapped EPR with 5,5-dimethylpyrroline-1-oxide (DMPO) was used to examine •OH produced in this process [45,46]. For bare carbon (A curve of Fig. 10), the signal of DMPO-adduct was very weak, but peaks appeared with loading 1.5 wt% Au (B curve of Fig. 10), and its intensity increased remarkably with increasing the Au content to 3.0 wt% (C curve of Fig. 10). With the same sample tube located in the resonant cavity and the identical composition of the DMPO-adduct solution, the intensity of EPR signal is dependent on the concentration of •OH [46]. Under the current reaction conditions, the system of SRAC/H_2O_2 did not generate •OH; it is consistent with the fact that no degradation of BPA was detected for the bare carbon. With the identical lineshape of DMPO-adduct among all these tested samples, the intensity can be directly related to the amount of OH• generated in the reaction system. The productivity of radicals increased with varying of the Au loading amount. We argue the interaction of Au nanoparticles on SRAC plays an important role in the creation of radicals.

Activated carbon has proved to possess unpaired electrons from dangling carbon atoms in the surface, which are normally located at the broken basal sites with relatively higher energy compared to the defects at edge sites of graphite sheets [47]. Those active sites are assumed to degrade the adsorbed H_2O_2 to form •OH [48]. Meanwhile, the complete basel site in graphite structure can scavenge the produced radicals immediately [49]. As a result, it is understandable that almost no •OH could be detected for the bare carbon (Fig. 10). It has been proposed that the dangling carbon atoms on the carbon surface are responsible for the adsorption of oxygen and H_2O_2 or activation of adsorbed metal atoms [47]. The binding energy between Au and the dangling bonds in graphite sheet is 2.4–2.6 eV [50].

In order to demonstrate the existence of dangling carbon atoms, the O_2-TPD spectra were obtained for both SRAC and Au(1.5 wt%)/SRAC. A desorption peak at 369 K was detected for the bare SRAC and shifted down to 213 K for Au(1.5 wt%)/SRAC; meanwhile the desorption amount of O_2 decreased from 230.0 to

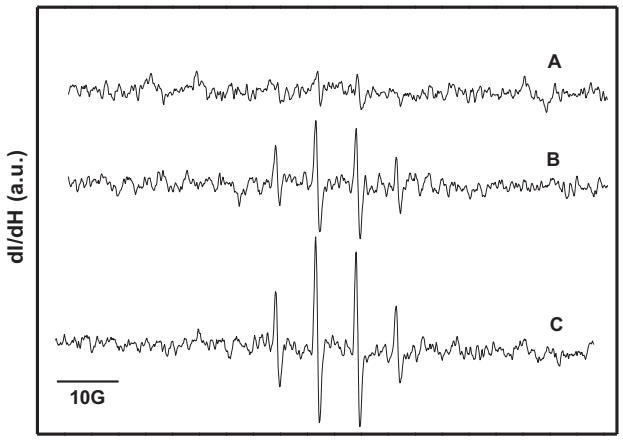

Fig. 10. DMPO-trapped EPR spectrums of SRAC (A), Au (1.5 wt%)/SRAC (B), and Au (3.0 wt%)/SRAC (C).

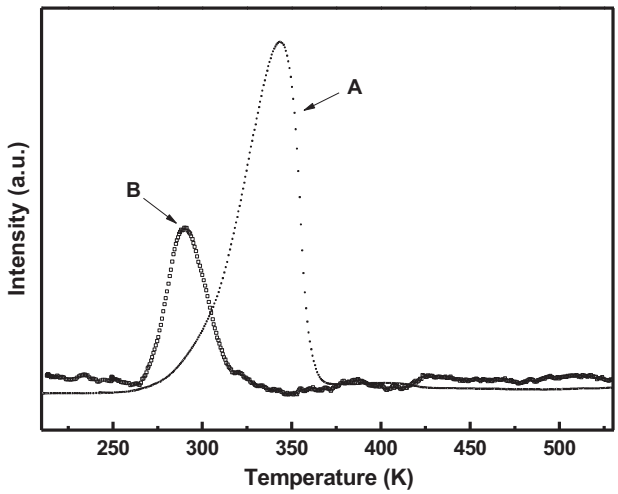

Fig. 11. O_2-TPD curves of as-prepared samples: SRAC (A) and Au(1.5 wt%)/SRAC (B).

68.8 cm^3/g (Fig. 11). We argue that O_2 should be adsorbed on carbon sites and/or at the interface since the adsorption of O_2 on the Au surface has not yet evidenced experimentally. The downshift of the peak and the decrease in the adsorption of oxygen after loading Au are probably due to the interaction between Au and dangling carbon atoms; while Au particles primarily take up the relatively higher energy sites.

We infer that the degradation of H_2O_2 should occur on Au atoms at the interface between Au nanoparticles and carbon; these sites should be enriched with dangling carbon atoms that Au atoms could be partially negatively charged or polarized. This hypothesis could be further supported by a recent study over a system of Au/silicon wafer, •OH from the decomposition of H_2O_2 was detected with doping Au atoms surrounding by Si-dangling bond [51].

The plausible pathway for the generation of •OH and the degradation of BPA are illustrated in Scheme 1. Generally, this process follows several steps: (1) Au atoms is partially charged or polarized due to unpaired electron in carbon substrate. (2) H_2O_2 is adsorbed and decomposed into •OH at the interface of Au particles and carbon; •OH is released from Au surface and reacted with BPA, which is perhaps weakly adsorbed on the catalyst surface. (3) The metallic Au^0 was reduced by H_2O_2 to $Au^{\delta-}$. In addition, other radicals, such as HOO• or O_2^{-}•, may be generated simultaneously during reaction. The detailed mechanistic study is underway.

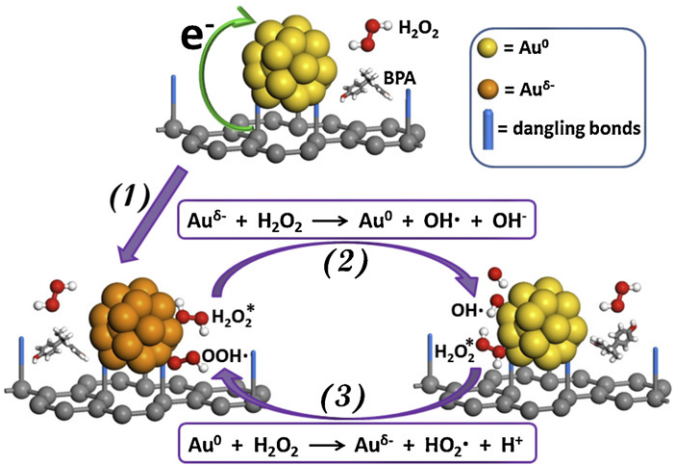

Scheme 1. The plausible mechanism for the generation of •OH in the Au-Fenton system.

4. Conclusions

In summary, Au/SRAC has proved to be effective Au-Fenton catalysts for the degradation of BPA by the production of OH•. It showed high activity and durability in a broad pH range (3.0–7.0) without extra energy input such as photon and electricity compared to other Au-Fenton catalysts. We believe the reported Au-Fenton system can be an excellent alternative for purifying drinking water, which may be contaminated with toxic and undegradable organic compounds. In this system, we tentatively attribute the generation of •OH to two factors: (1) Au atoms are polarized or negatively charged on the carbon surface, which is abundant of dangling bonds; (2) there is few complete basel sites or other sites to scavenge •OH. This work could inspire further study regarding degradation of toxic organic compounds using this simply and stable Au-Fenton system.

Acknowledgments

The authors are grateful to the support from the Chinese Education Ministry 111 project (B08021), the National Natural Science Foundation of China (21006068, 21176071, 21106041, 21273070), Shanghai PuJiang Talent Program (2011/11PJ1402400), the Program for New Century Excellent Talents in University (NCET-10-0611), the Program of Introducing Talents of Discipline to Universities (B06006) for financial support, Innovation Program of Shanghai Municipal Education Commission (11ZZ52, 12ZZ051), Science and Technology Commission of Shanghai Municipality (11JC1402700).

References

[1] F.S. vom Saal, B.T. Akingbemi, S.M. Belcher, L.S. Birnbaum, D.A. Crain, M. Eriksen, F. Farabollini, L.J. Guillette Jr., R. Hauser, J.J. Heindel, S.-M. Ho, P.A. Hunt, T. Iguchi, S. Jobling, J. Kanno, R.A. Keri, K.E. Knudsen, H. Laufer, G.A. LeBlanc, M. Marcus, J.A. McLachlan, J.P. Myers, A. Nadal, R.R. Newbold, N. Olea, G.S. Prins, C.A. Richter, B.S. Rubin, C. Sonnenschein, A.M. Soto, C.E. Talsness, J.G. Vandenbergh, L.N. Vandenberg, D.R. Walser-Kuntz, C.S. Watson, W.V. Welshons, Y. Wetherill, R.T. Zoeller, Reprod. Toxicol. 24 (2007) 131–138.
[2] G.O. Noonan, L.K. Ackerman, T.H. Begley, J. Agric. Food Chem. 59 (2011) 7178–7185.
[3] G.M. Klečka, C.A. Staples, K.E. Clark, N. van der Hoeven, D.E. Thomas, S.G. Hentges, Environ. Sci. Technol. 43 (2009) 6145–6150.
[4] C. Liao, K. Kannan, Environ. Sci. Technol. 45 (2011) 6761–6768.
[5] J. Oehlmann, M. Oetken, U. Schulte-Oehlmann, Envrion. Res. 108 (2008) 140–149.
[6] L.N. Vandenberg, M.V. Maffini, C. Sonnenschein, B.S. Rubin, A.M. Soto, Endocr. Rev. 30 (2009) 75–95.
[7] C.A. Staples, P.B. Dome, G.M. Klecka, S.T. Oblock, L.R. Harris, Chemosphere 36 (1998) 2149–2173.
[8] N. Diano, V. Grano, L. Fraconte, P. Caputo, A. Ricupito, A. Attanasio, M. Bianco, U. Bencivenga, S. Rossi, I. Manco, L. Mita, G. Del Pozzo, D.G. Mita, Appl. Catal. B 69 (2007) 252–261.
[9] I. Bautista-Toledo, M.A. Ferro-García, J. Rivera-Utrilla, C. Moreno-Castilla, F.J. Vegas Fernández, Environ. Sci. Technol. 39 (2005) 6246–6250.
[10] B. Gözmen, M.A. Oturan, N. Oturan, O. Erbatur, Environ. Sci. Technol. 37 (2003) 3716–3723.
[11] Y.-P. Chin, P.L. Miller, L. Zeng, K. Cawley, L.K. Weavers, Environ. Sci. Technol. 38 (2004) 5888–5894.
[12] Z.-h. Liu, Y. Kanjo, S. Mizutani, Sci. Tot. Environ. 407 (2009) 731–748.
[13] Z. Guo, R. Feng, J. Hazard. Mater. 163 (2009) 855–860.
[14] J. Lee, H. Park, J. Yoon, Environ. Technol. 24 (2003) 241–248.
[15] X. Shao, J. Ma, G. Wen, J. Yang, Chin. Sci. Bull. 55 (2010) 802–808.
[16] J. Jiang, S.-Y. Pang, J. Ma, Environ. Sci. Technol. 44 (2010) 4270–4275.
[17] J.J. Pignatello, E. Oliveros, A. MacKay, Crit. Rev. Environ. Sci. Technol. 36 (2006) 1–84.
[18] F. Haber, J. Weiss, Proc. Roy. Soc. Lond., Math. Phys. Sci. 147 (1934) 332–351.
[19] C. Walling, Acc. Chem. Res. 8 (1975) 125–131.
[20] E. Neyens, J. Baeyens, J. Hazard. Mater. 98 (2003) 33–50.
[21] P. Bautista, A.F. Mohedano, J.A. Casas, J.A. Zazo, J.J. Rodriguez, J. Chem. Technol. Biotechnol. 83 (2008) 1323–1338.
[22] M. Hartmann, S. Kullmann, H. Keller, J. Mater. Chem. 20 (2010) 9002–9017.

[23] A. Dhakshinamoorthy, S. Navalon, M. Alvaro, H. Garcia, ChemSusChem 5 (2012) 46–64.
[24] C. Nozaki, C.G. Lugmair, A.T. Bell, T.D. Tilley, J. Am. Chem. Soc. 124 (2002) 13194–13203.
[25] M. Haruta, N. Yamada, T. Kobayashi, S. Iijima, J. Catal. 115 (1989) 301–309.
[26] G.J. Hutchings, J. Catal. 96 (1985) 292–295.
[27] G.J. Hutchings, M. Haruta, Appl. Catal. A 291 (2005) 2–5.
[28] J.K. Edwards, B.E.N.N. Solsona, A.F. Carley, A.A. Herzing, C.J. Kiely, G.J. Hutchings, Science 323 (2009) 1037–1041.
[29] M.S. Chen, D.W. Goodman, Science 306 (2004) 252–255.
[30] X.-L. Du, L. He, S. Zhao, Y.-M. Liu, Y. Cao, H.-Y. He, K.-N. Fan, Angew. Chem. Int. Ed. 50 (2011) 7815–7819.
[31] I.X. Green, W. Tang, M. Neurock, J.T. Yates, Science 333 (2011) 736–739.
[32] Y. Lee, G. He, A.J. Akey, R. Si, M. Flytzani-Stephanopoulos, I.P. Herman, J. Am. Chem. Soc. 133 (2011) 12952–12955.
[33] A. Wittstock, V. Zielasek, J. Biener, C.M. Friend, M. Bäumer, Science 327 (2010) 319–322.
[34] J. Gong, C.B. Mullins, J. Am. Chem. Soc. 130 (2008) 16458–16459.
[35] Y.-F. Han, N. Phonthammachai, K. Ramesh, Z. Zhong, T. White, Environ. Sci. Technol. 42 (2007) 908–912.
[36] S. Navalon, R. Martin, M. Alvaro, H. Garcia, Angew. Chem. Int. Ed. 49 (2010) 8403–8407.
[37] S. Navalon, M. de Miguel, R. Martin, M. Alvaro, H. Garcia, J. Am. Chem. Soc. 133 (2011) 2218–2226.
[38] R. Martín, S. Navalon, M. Alvaro, H. Garcia, Appl. Catal. B 103 (2011) 246–252.
[39] S. Navalon, R. Martin, M. Alvaro, H. Garcia, ChemSusChem 4 (2011) 650–657.
[40] Z. Liu, L. Ling, W. Qiao, L. Liu, Carbon 37 (1999) 663–667.
[41] Y. Meng, D. Gu, F. Zhang, Y. Shi, L. Cheng, D. Feng, Z. Wu, Z. Chen, Y. Wan, A. Stein, D. Zhao, Chem. Mater. 18 (2006) 4447–4464.
[42] B.P. Block, J.C. Bailar, J. Am. Chem. Soc. 73 (1951) 4722–4725.
[43] I.R. Cohen, T.C. Purcell, A.P. Altshuller, Environ. Sci. Technol. 1 (1967) 247–252.
[44] G.V. Buxton, C.L. Greenstock, W.P. Helman, A.B. Ross, J. Phys. Chem. Ref. Data 17 (1988) 513–886.
[45] I. Yamazaki, L.H. Piette, J. Am. Chem. Soc. 113 (1991) 7588–7593.
[46] M.A. Voinov, J.O.S. Pagaïn, E. Morrison, T.I. Smirnova, A.I. Smirnov, J. Am. Chem. Soc. 133 (2010) 35–41.
[47] J. Phillips, B. Xia, J.A. Menéndez, Thermochim. Acta 312 (1998) 87–93.
[48] A. Rey, J.A. Zazo, J.A. Casas, A. Bahamonde, J.J. Rodriguez, Appl. Catal. A 402 (2011) 146–155.
[49] I. Fenoglio, M. Tomatis, D. Lison, J. Muller, A. Fonseca, J.B. Nagy, B. Fubini, Free Radic. Biol. Med. 40 (2006) 1227–1233.
[50] J. Akola, H. Häkkinen, Phys. Rev. B 74 (2006) 165404.
[51] T. Ramalho, H. Carvalho, A. Batista, C. Pérez, A. Gobbi, J. Mater. Sci. 44 (2009) 1029–1034.